Tannic-acid-mediated synthesis and characterization of magnetite-gold nanoplatforms for photothermal therapy

Tannic acid mediated synthesis and characterization of magnetite-gold nanoplatforms for photothermal therapy

Marta Miola*[1], Cristina Multari[1], Nina Kostevšek [2], Roberto Gerbaldo[1], Francesco Laviano[1], Enrica Verné[1]

[1] Department of Applied Science and Technology, Politecnico di Torino, corso Duca degli Abruzzi 24, 10129 Torino, Italy

[2] Department for nanostructured materials, Jožef Stefan Institute, Jamova 39, 1000 Ljubljana, Slovenia

*corresponding authors marta.miola@polito.it

Politecnico di Torino

Department of Applied Science and Technology, Politecnico di Torino, Torino (TO), Italy

Institute of Materials Engineering and Physics

Corso Duca degli Abruzzi, 24 - 10129 (TORINO) ITALY

Tel: +39 0110904717

Abstract

Magnetite (MNPs) and gold (GNPs) nanoparticles attracted attention because of their potentialities in cancer treatment. In this paper, an original synthesis of MNPs and GNPs was designed through the innovative use of tannic acid (TA), which allows the synthesis and the stabilization of eco-friendly hybrid nanoplatforms (HNPs) avoiding toxic chemicals. HNPs were characterized in terms of size, morphology, composition, magnetic and plasmonic properties, ability to generate heating under laser irradiation and their

hemotoxicity. The results revealed that the TA allowed the production of HNPs through a new, simple and green synthesis method. The HNPs preserved the peculiar properties of each nanomaterial, and did not show any hemotoxic effect, thus representing an innovative approach for magneto-photothermal therapy of cancer.

Structured Abstract

Aim: the design of new hybrid nanoplatforms (HNPs) through the innovative and eco-friendly use of tannic acid (TA) for the synthesis and the stabilization of the NPs.

Materials & Methods: the size, morphology, composition as well as magnetic and plasmonic properties of HNPs were investigated together with their ability of HNPs to generate heating under laser irradiation and the hemotoxicity to explore their potential use for biomedical applications.

Results and Conclusions: the use of TA allowed the synthesis of the HNPs by adopting a simple and green method. The HNPs preserved the peculiar properties of both magnetic and plasmonic nanoparticles and did not show any hemotoxic effect.

Keywords

Magnetite nanoparticles; gold nanoparticles; magneto-plasmonic nanoparticles; phothermal therapy; tannic acid;

1. Introduction

In recent years, many studies have been focused on new applications of nanotechnology in biomedical field. Nowadays one of the main applications of nanotechnology in

biomedicine is the use of nanoparticles [1-7]. In particular, magnetite and gold nanoparticles (MNPs and GNPs respectively) have attracted a lot of interest in the scientific community thanks to the possibility to use them in different research fields [8-14]. MNPs have been considered as contrast agents for magnetic resonance imaging, heat sources for hyperthermia and vectors for drug delivery, especially in cancer therapy [15-21]. Moreover, they show low toxicity, high biocompatibility and great stability [22]. GNPs have attracted huge interest due to their easiness of synthesis and surface modification, high stability and excellent biocompatibility; in fact, they present very low toxicity even at high concentration [10-23]. Furthermore, GNPs possess a unique photo-physical phenomenon which is not present in massive metal: localized surface plasmon resonance (LSPR) [11,24-26]. The LSPR effect is the result of the nanoparticles interaction with light radiation in a specific wavelength, in fact, GNPs are able to transform the received light into thermal energy by producing heat. This could bring the cancer cells to apoptosis as a consequence of their high heat sensitivity [27]. Thus, GNPs are one of the most promising tools for photothermal therapy [11].

Combining MNPs and GNPs together, is possible to create a hybrid nanoplatform which preserves the specific properties of each nanomaterial, thus creating an innovative approach for magneto-photothermal therapy of cancer [28]. Indeed, magnetoplasmonic HNPs could be driven in a specific tumour site due to their ability to be activated through an external magnetic field while acting as photothermal system by exploiting the SPR effect when irradiated with a laser light. Moreover, it has been recently reported that the combined magnetic and optical properties of magneto-plasmonic HNPs could be successfully exploited in multimodal imaging techniques [29].

The aim of this work is to synthetize MNPs and GNPs creating a magneto-plasmonic nanoplatform (HNPs) through an innovative and eco-friendly synthesis of GNPs, which

uses tannic acid (TA) as the unique reagent able, at the same time, to reduce GNPs and stabilize HNPs without using any other toxic chemicals. This method faces up to the need to develop more environmentally friendly approaches in order to avoid the problems that chemical and physical NPs synthesis procedures usually present, such as the use of toxic chemicals that can lead to both health and environmental issues as well as the high exposure risk of the operator [30,31]. This new awareness can be achieved by using a wide range of biological resources, which could bring various advantages in the NPs synthesis, such as simplicity, low-cost, non-toxic procedures and compatibility for biomedical and pharmaceutical applications [32,33].

Tannic acid was selected since it is a polyphenolic compound extracted from plants [34] and can be used as stabilizing and reducing agent [12,35] avoiding the use of all other hazardous chemicals, creating a green and non-toxic synthesis of HNPs [36]. Moreover, TA is well known for its natural antioxidant, anti-inflammatory, antitumoral and antimicrobial properties [37,38]. This organic compound was used to allow GNPs nucleation directly on MNPs surface due to its high reducing power [36]. Furthermore, working under mild-acidic/basic condition, a partial hydrolyzation of TA take place generating glucose and gallic acid [39]: the glucose guarantee the property of being a good stabilizing agent while the gallic acid induces the formation of GNPs at room temperature thanks to its well-known reducing power [39,40].

A further aim of this work is to characterize the synthetized HNPs from different points of view, including size, morphology, composition, magnetic and plasmonic properties, ability to generate heating under laser irradiation. Moreover, it is well known that NPs can easily access blood cells, influencing their function and resulting in potentially toxic effects [41]. Therefore, a preliminary study on hemotoxicity of HNPs in contact with red

blood cells has been performed to attest the possibility to use the newly engineered nanoplatforms for biomedical applications.

2. Materials and methods

2.1 HNPs synthesis

HNPs were prepared by improving a synthesis route reported in our previous papers [12,35]. The syntheses differ from each other because in the previous ones the MNPs were stabilized with citric acid and functionalized with APTES (3-Aminopropyl-triethoxysilane) to promote the GNPs attachment, while in the synthesis here described, the TA was used as unique benign reagent that works both as stabilizing and reducing agent. Briefly, Fe_3O_4 NPs were firstly synthetized by the co-precipitation method in which 37.5 ml of 0.1 M $FeCl_2$ and 50 ml of 0.1 M $FeCl_3$ were mixed together until the salts were completely dissolved. To induce the magnetite formation, NH_4OH was added drop by drop until the pH reached a value of 9.5 and the suspension turned black, indicating the precipitation of MNPs. Then the suspension was sonicated in an ultrasonic bath (SONICA Ultrasonic Cleaner) for 20 minutes and washed two times before re-suspended in 100 ml of bi-distilled water [42,43].

TA solution was prepared by dissolving 2.55 mg of TA in 1.2 ml of bi-distilled water and buffered at pH= 8 in order to improve its reducing power. Then the TA solution was added to the MNPs dispersion with a ratio TA(ml) : MNPs(ml) of 0.3 and left at 70 °C for 5 minutes under agitation to allow the TA binding on NPs. All the steps were carried out rapidly in order to avoid the Fe_3O_4 NPs aggregation. Finally, 60 mg of $HAuCl_4$ were dissolved in 12 ml of bi-distilled water and added to the TA-MNPs suspension and left under continuous stirring at 70 °C for 5 minutes. This step would allow the GNPs nucleation directly on MNPs surface. All the reactants were purchased by Sigma Aldrich®.

The obtained HNPs were then characterized in terms of size, morphology, composition, magnetic and plasmonic properties. Figure 1 reports schematically the above-mentioned synthesis steps.

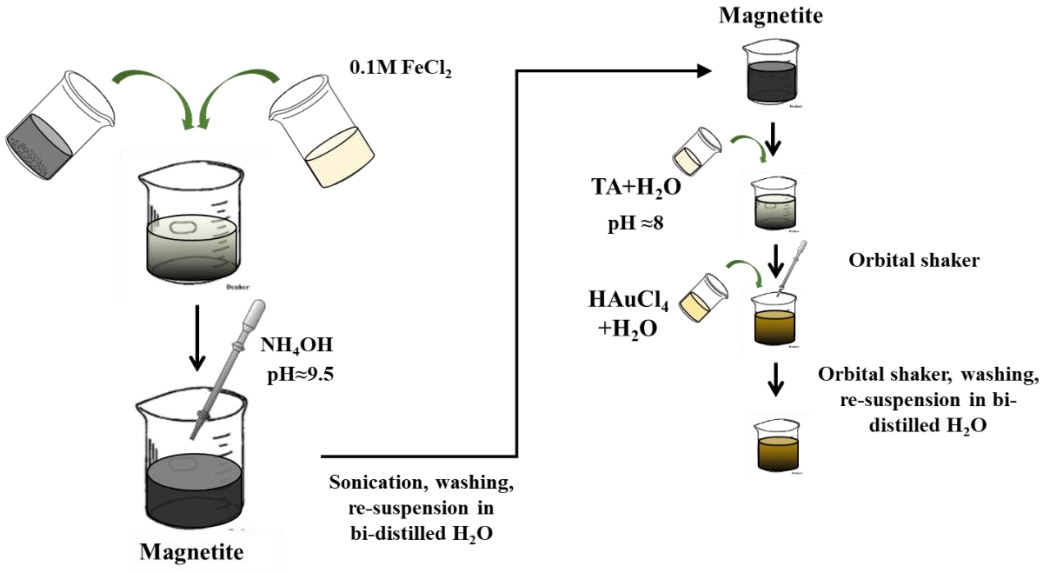

Figure 1. Experimental procedure for the HNPs synthesis.

2.2 HNPs characterization

2.2.1 Morphological and compositional characterization

In order to assess the dimension, the shape and the morphology of the as-synthetized HNPs, electron microscopes FESEM (Zeiss supra 40 GEMINI Field Emission Scanning Electron Microscopy) and - TEM (FEI Tecnai F20 TWIN transmission electron microscope with a Schottky emitter operated at 200 KV) were used; the chemical composition and the correct reduction of GNPs on MNPs were detected by Zeiss supra 40 GEMINI X-ray spectroscopy (EDS). For these analyses 5µl of sample solution were placed on a Lacey carbon coated 200 mesh copper grid and then located on the appropriate support for the analysis.

To verify the effective functionalization and perform elemental analysis a JASCO 4000 Fourier transform infrared spectroscopy (FT-IR) was used, spectra were acquired from

4000 to 500 cm^{-1}, to perform FT-IR analysis, the solution was left at room temperature until the powder were completely dried.

2.2.2 Optical characterization

The UV-Visible spectrophotometry, UV-2600 Shimadzu (UV-VIS) was employed to identify at which wavelength the HNPs are able to absorb and to provide information on their size and aggregation, for this analysis the HNPs were maintained in their original water suspension.

2.2.3 Magnetic characterization

The magnetic properties of HNPs were investigated by means of a DC magnetometer (LakeShore 7225) equipped with a Cryogen-Free Magnet, useful to study the superparamagnetic behavior of the MNPs and the ability of the sample to be activated with an external magnetic field by means of an induction heating system (FELMI-EGMA 6-10.15 REV.01). Magnetic hysteresis cycle measurements were performed at room temperature in quasi static condition using an applied magnetic field up to 800 kA/m using the samples in form of powder.

2.2.4. Plasmonic behavior under laser irradiation

The HNPs were subjected to a 10 minutes NIR laser irradiation of 808 nm (model FC-808, CNI Optoelectronics Tech, Changchun, China) in order to detect their ability to be activated with an external light stimulus and exploit their SPR effect of increasing temperature. The HNPs concentration used for the analysis was 0.1 mg/ml (determined using ICP-MS analysis) in a total volume of 1 ml. The laser power used was set at 1 W/cm^2 and the spot size of the laser beam was 1 cm in order to irradiate the entire volume of the

vial. Temperature of the samples was monitored in real time using a J-type Teflon thermocouple.

This analysis is useful to study their ability to be used as photothermal agent in cancer treatment, for this reason, the HNPs were maintained in their original water suspension.

2.2.5 In-vitro hemotoxicological analysis

Once attested all the physical, chemical, magnetic and optical properties, a preliminary in-vitro cytotoxicity evaluation of the as-produced HNPs was performed, in which a nanoplatforms concentration of 35 and 100 μg/ml (determined via ICP-MS analysis) were put in contact with red blood cells for 5 hours.

For the hemolysis study, red blood cells were isolated from the whole sheep blood, supplied by the Veterinary Faculty (University of Ljubljana, Slovenia) in Alsever's medium (TCS Biosciences Ltd, UK) and used within one week. Red blood cells were isolated via centrifugation (2500 rpm/10 min) and washed 3-times with phosphate-buffered saline (PBS) buffer (tablets, Sigma Aldrich). Nanoparticles suspended in PBS were incubated with 5 vol.% of red blood cells (pH 7.4) for 5 h at 37 °C with constant orbital shaking in 1.5 ml tubesEppendorfof, Germany, volume of samples 1 mL, all samples in triplicates). After incubation, tubes were centrifuged (1500 rpm/4 min) to sediment cells and supernatant was analyzed in triplicates. Hemolysis was evaluated by measuring released hemoglobin absorbance (A) at 541 nm using a plate reader (Synergy H4, BioTek, Winooski, VT, USA). Samples representing positive control (100% dead) were prepared by lysing control samples with deionized water via hypotonic osmotic shock. Percent hemolysis was then calculated as follows: Hemolysis (%)=100·(Asample – Acontrol)/(A100% dead – Acontrol). One-way ANOVA and Student's t-test was used for our statistical analysis. The data were presented as mean ± SD for all experiments.

3. Results and discussion

In this paragraph, the morphological, compositional and chemical characterizations concerning the HNPs are described. In particular, a preliminary characterization on bare iron oxide nanoparticles was firstly performed in order to verify the correct formation of MNPs followed by the analyses achieved to attest the correct binding of TA on MNPs.

To verify the size and morphology of MNPs, they were firstly characterized by means of TEM analysis. In figure 2 TEM images of bare iron oxide nanoparticles are shown, in which is visible their pseudo-spherical shape and a dimensional range between 5-15 nm.

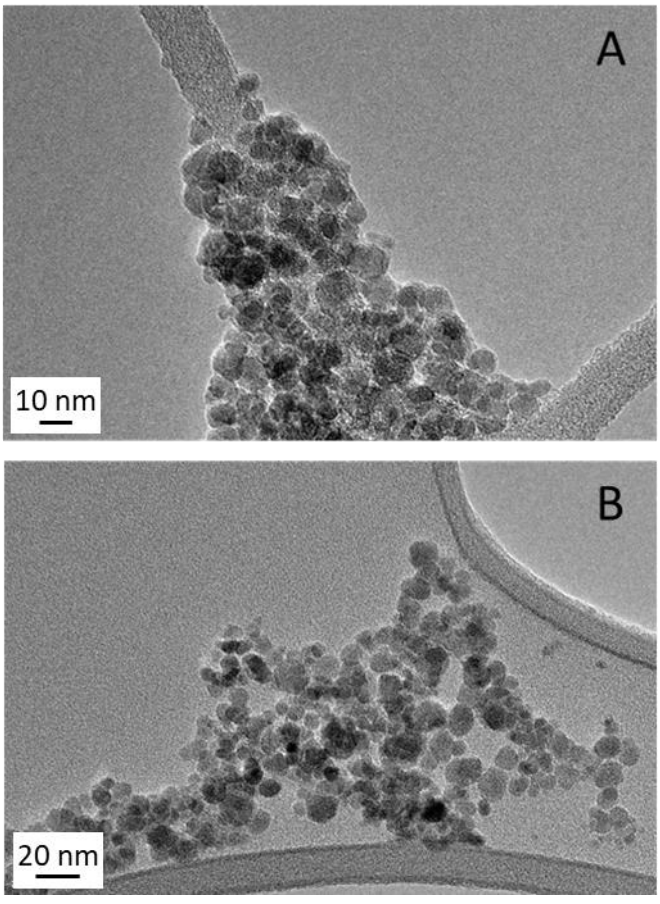

Figure 2: TEM image of MNPs. Scale bar: figure A 10 nm; figure B 20 nm

In order to confirm the correct binding of TA on MNPs surface, the FT-IR and UV-Vis analyses were performed as shown in figure 3 and figure 4 respectively. In FT-IR graph

(figure 3), the patterns of MNPs and TA functionalized MNPs are shown. Both spectra display the strong vibrational modes of Fe-O bonds of magnetite located at 585 cm^{-1} [44,45], while from the TA-MNPs pattern (red line) the main characteristic peaks of TA [46] are visible, in particular, the 758 cm^{-1} peak indicates out of plane CH bending of phenyl groups, the peak at 923 cm^{-1} is referred to OH out of plane bending of acid groups, the C=O stretching vibration at 1730-1705 cm^{-1} and C-O at 1100-1300 cm^{-1}, while around 1452 cm^{-1} the stretching vibrations of -C-C aromatic groups appear. Moreover, as confirmation of correct functionalization of MNPs with TA, the broad peak at 3400 cm^{-1}, which represent the hydroxyl groups and surface-adsorbed water molecules, is visible together with the vibrational modes of Fe-O bonds of magnetite

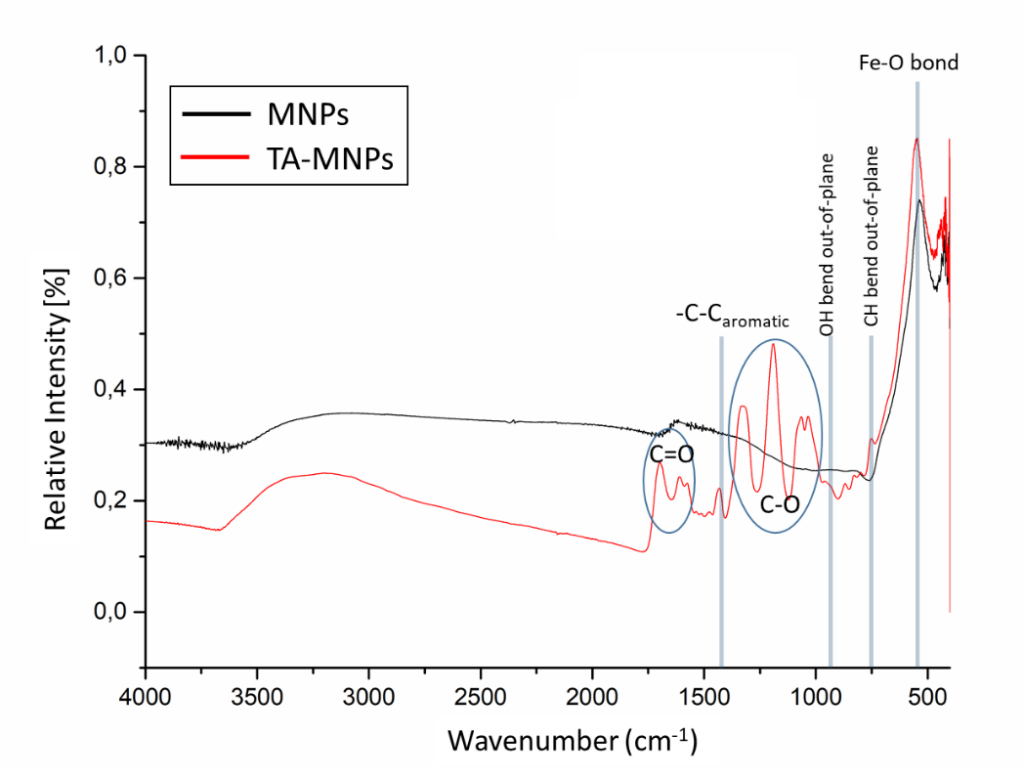

Figure 3: FTIR spectra of MNPs and TA-MNPs

Figure 4 reports the UV-Vis analysis in which the peak associated to the tannic acid at around 300 nm is visible. This result corroborates the outcomes obtained from FT-IR and confirms the correct binding of tannic acid on MNPs surface, thus confirming that TA can be grafted onto the surface of magnetic particles, without interposing other spacer molecules (e.g. APTES).

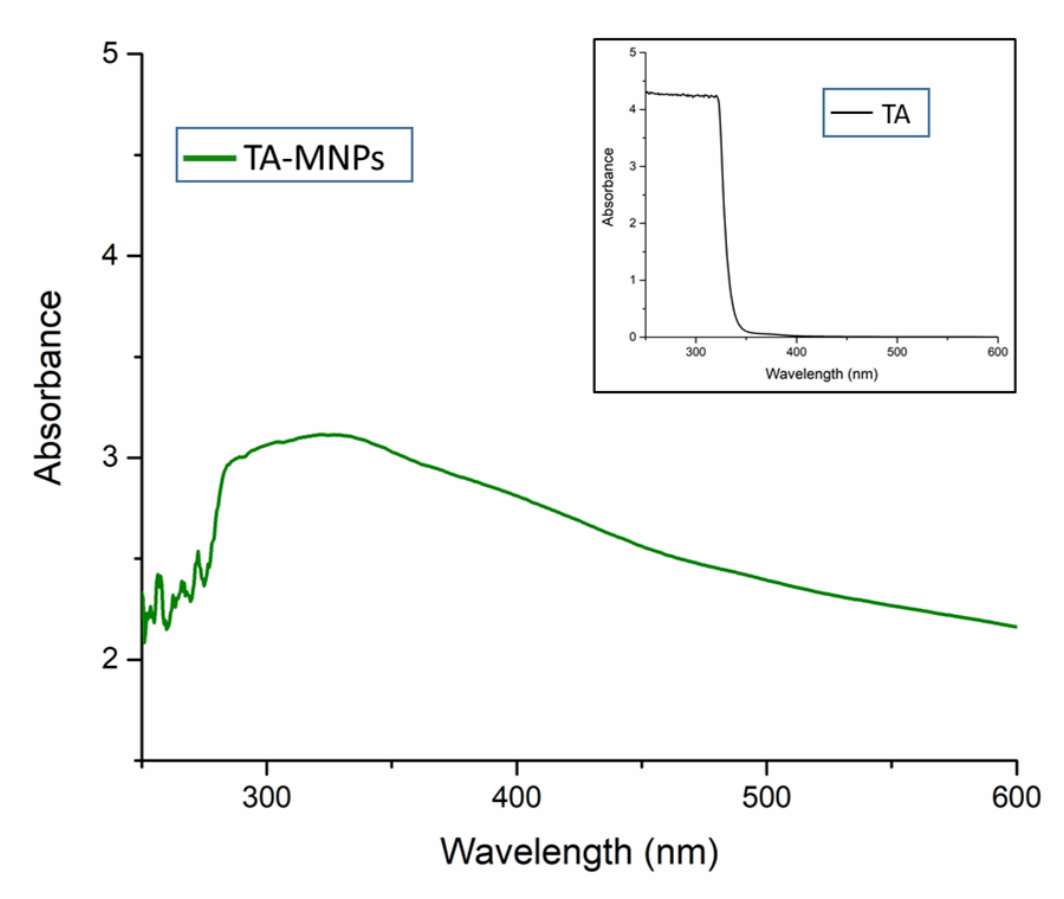

Figure 4: UV-Vis spectra of TA-MNPs. In the inset: UV-Vis spectra of TA alone.

Once attested the correct functionalization with TA, the TEM analysis was used to verify the size and morphology of HNPs, as well as to attest the correct attachment of GNPs on iron oxide core. Figure 5 shows the TEM images of HNPs, in which the GNPs are visible; they appear darker than MNPs due to their higher atomic number and electron density. GNPs show an approximately spherical shape and a dimension around 10-20 nm,

confirming the presence of GNPs on MNPs core creating a sort of nano-dumbbell structures.

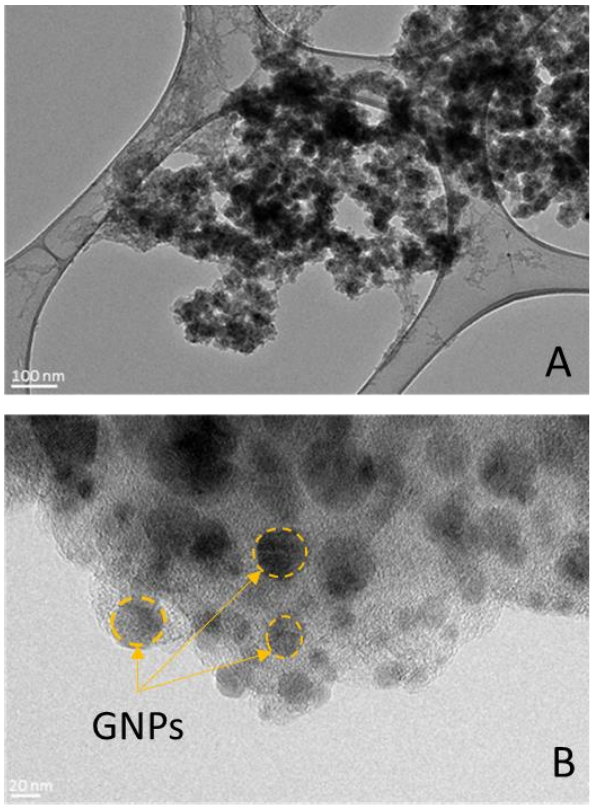

Figure 5: TEM image of HNPs. In figure 4 (B) GNPs are evidenced. Scale bar: figure A 100 nm; figure B 20 nm.

In figure 6 the STEM images acquired in dark field mode are shown, in which high mass materials (such as gold) appear bright. The figure shows the morphological aspect of HNPs, in which the GNPs result to be homogeneous and well-dispersed on magnetite surface. This analysis corroborates the TEM results previously obtained, in which it is possible to observe a high concentration of GNPs attached to the MNPs with a dimensional range between 10 nm and 20 nm. The correct reduction of GNPs on MNPs is also supported by the EDS analysis (figure 7), that evidence the presence of all the elements characteristic of MNPs and GNPs.

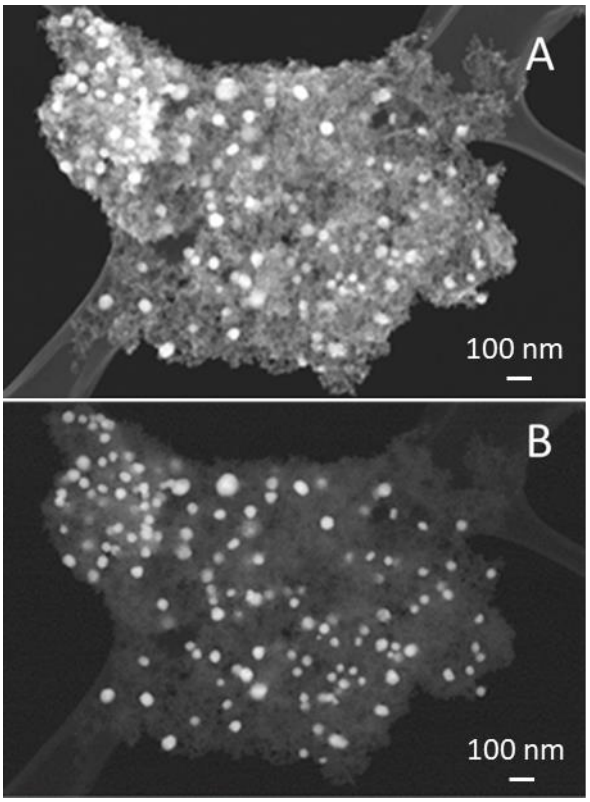

Figure 6: STEM images of HNPs. Scale bar: 100 nm.

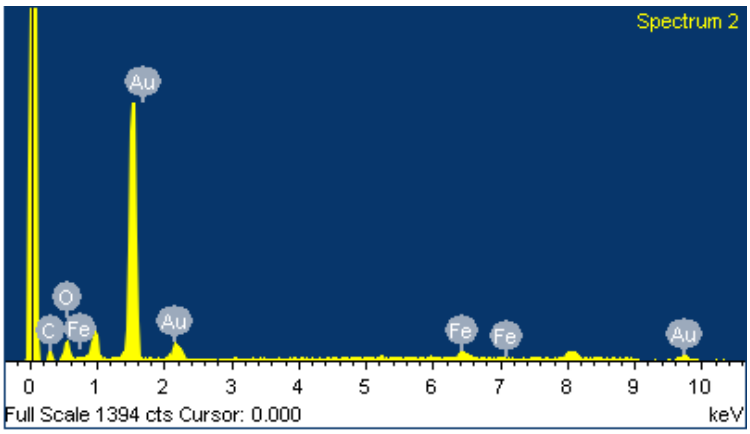

Figure 7: EDS analysis of HNPs.

Moreover, in order to identify the functional groups present in the TA, which is responsible for the reduction of GNPs and stabilization of HNPs, FT-IR measurement of the final HNPs solution was carried out as shown in figure 8. In the image it is possible to

observe an altered intensity and position of the TA peaks with respect to the FT-IR of TA-MNPs (figure 3) as indication of the correct reduction of GNPs. In particular, the shift of the broad peak from 3400 cm^{-1} to lower wavenumber suggests the involvement of OH functional groups in the reduction process as well as the altered intensity of CO groups and C-C aromatic rings, which indicate the involvement of TA-MNPs in immobilization of GNPs (47). On the basis of data, it could be inferred that the TA remains bound to the HNPs surface and that the TA phenolic hydroxyls may be responsible for the reduction of metal ions. During the metal reduction process, the COO- group present in the TA, together with the rest of the molecule, can works as surfactant on the HNPs surface stabilizing them through electrosteric stabilization (48).

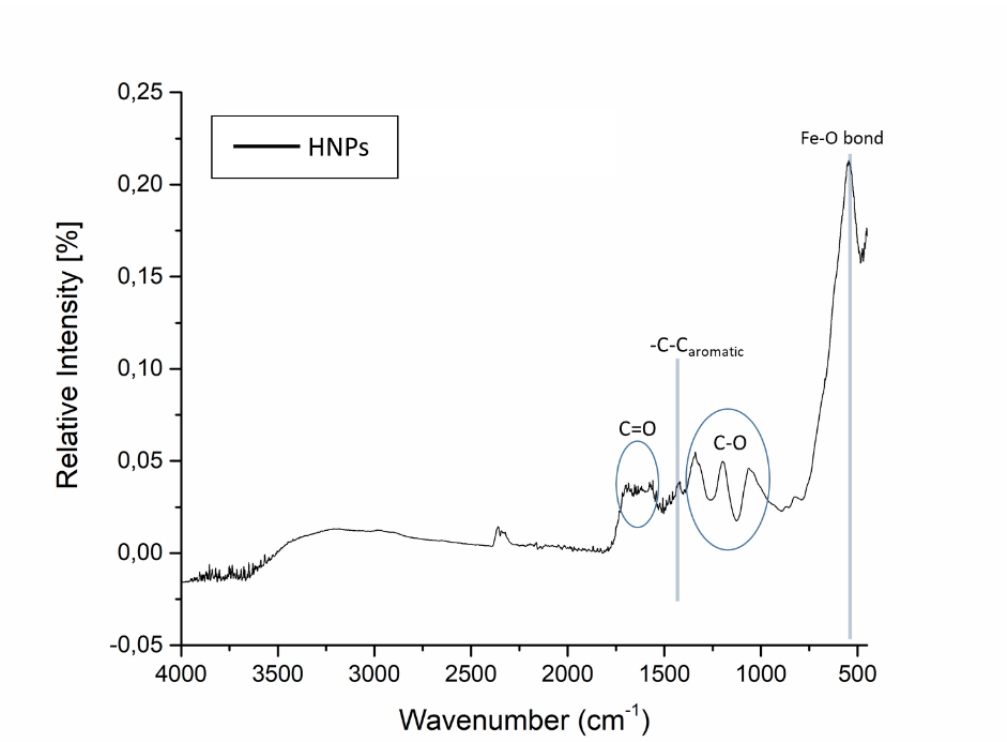

Figure 8: FT-IR spectra of HNPs

Once attested the correct HNPs formation and the correct role of TA to work as reducing and stabilizing agent, the UV-Visible spectrophotometry was employed to identify at

268 which wavelength the HNPs are able to absorb. The graph in figure 9 shows a high signal
269 in the GNPs absorbing window with sharp absorbing peak at 620 nm. This analysis is
270 useful to attest the great ability of GNPs to absorb light as well as to confirm the high
271 concentration, homogeneous dimension and very good dispersion of GNPs in the solution
272 [11]: this is confirmed by the broad gold extinction peak which in case of aggregation it
273 would show a decrease in intensity (due to the depletion of stable nanoparticles) and a
274 wider peak towards longer wavelengths (due to the formation of aggregates) [49].
275
276

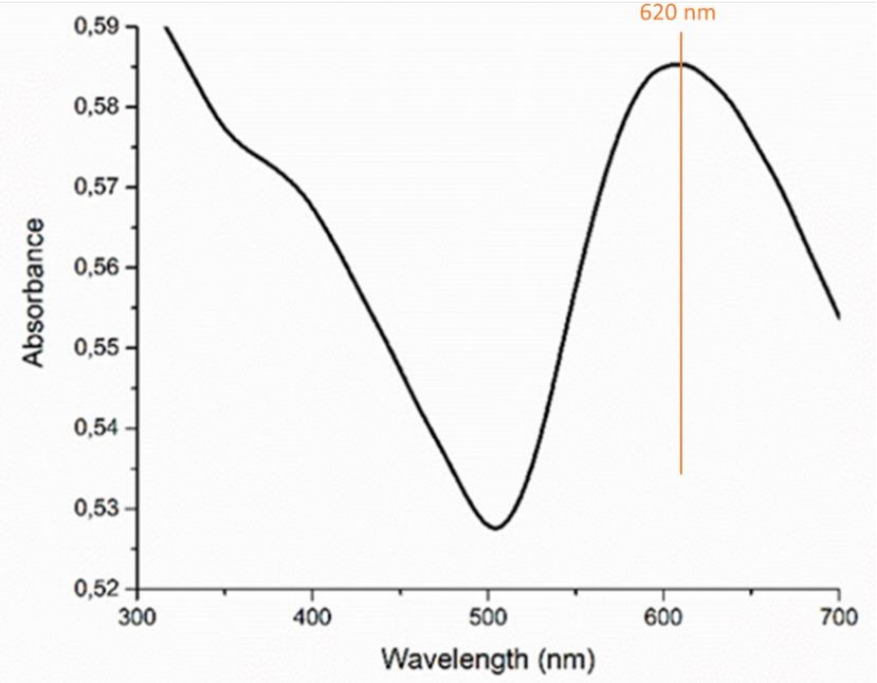

277
278 **Figure 9**: UV-Vis of HNPs.

279
280 With the aim to determine the effect that GNPs have on the magnetic properties of pure
281 MNPs, the magnetic properties of the suspension were evaluated by means of
282 magnetization measurements system and induction heating system. In fact, it is important

to consider that the ability to manage the HNPs using a magnetic field is one of the main reasons for utilizing Fe_3O_4 NPs as support for GNPs.

In particular, in figure 10 magnetic hysteresis cycle curves at room temperature of bare MNPs (black curve) and the as synthetized HNPs (pink curve) are reported. Here it is possible to observe that both the samples exhibit a superparamagnetic behaviour as confirmed by the negligible coercive field and remanence magnetization [50]. The higher magnetization values of MNPs with respect to HNPs, could be linkable to its lack of any additional element that lower these properties (such as the TA and GNPs); in fact, the decrease in the saturation magnetizations of HNPs, could be due to the diamagnetic nature of GNPs anchored on MNPs surface, as well as the minor amount of magnetic NPs in the sample in which gold is also present. Despite this, the HNPs show no hysteresis, indicating that GNPs are not influencing excessively the magnetic properties of the precursor [51].

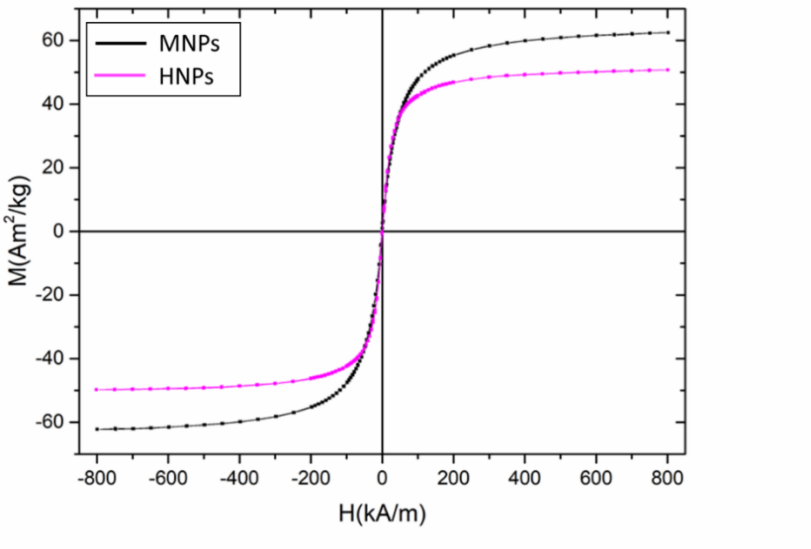

Figure 10: Magnetic hysteresis cycles of MNPs and HNPs.

In figure 11, the temperature-time curves obtained by submitting the samples to an external magnetic field are reported. This analysis is useful to attest the ability of the

sample to be activated with an external mediator. In particular, it is possible to notice that MNPs (black curve) are able to produce higher heating than HNPs (red curve), due to the same reasons for which the magnetization appeared lower in figure 10. Despite this, the synthetized HNPs are able to be externally activated with the applied magnetic field: this means that the GNPs decoration is not influencing the magnetic properties of HNPs, corroborating the magnetization measurement results previously obtained.

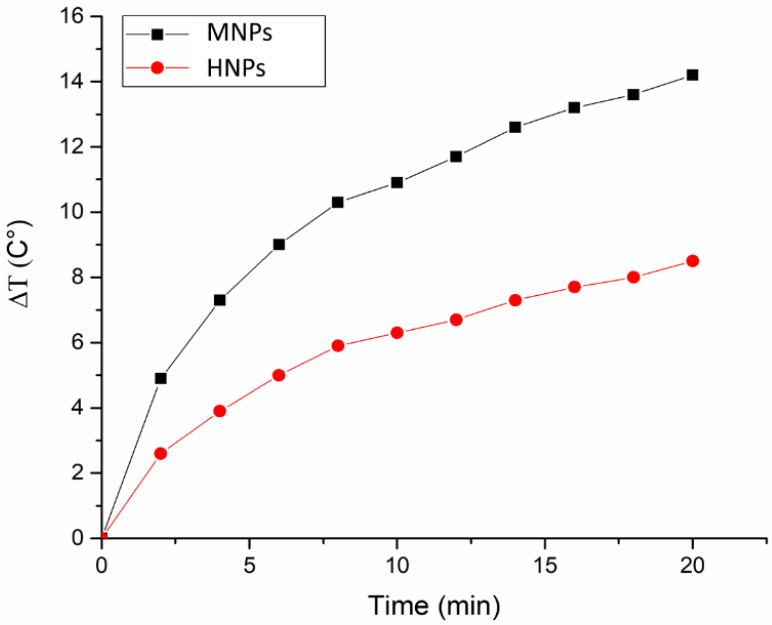

Figure 11: Temperature-Time curve of MNPs and HNPs after 20 min of an external magnetic field application. Applied magnetic field: 800 kA/m.

Finally, the HNPs were subjected to a laser irradiation in order to detect their ability to be activated with an external light stimulus and to exploit their SPR effect increasing their temperature. This analysis is useful to study their ability to be used as photothermal agent in cancer treatment. The same test was performed both with HNPs dispersed in water at

concentration of 0.1 mg/ml than with only water, to observe the difference between the two solutions. In figure 12, it is visible that after 10 minutes of laser irradiation, the HNPs are able to raise a temperature of 40/45°C ascribable to the high absorption spectra of GNPs at the characteristic wavelength of the irradiation showed in UV-Vis graph (figure 9), while, as expected, the water is not showing any effect when irradiated. This result confirms the excellent ability of GNPs to exploit SPR effect demonstrating the ability of the synthetized HNPs to be used in photothermal therapy.

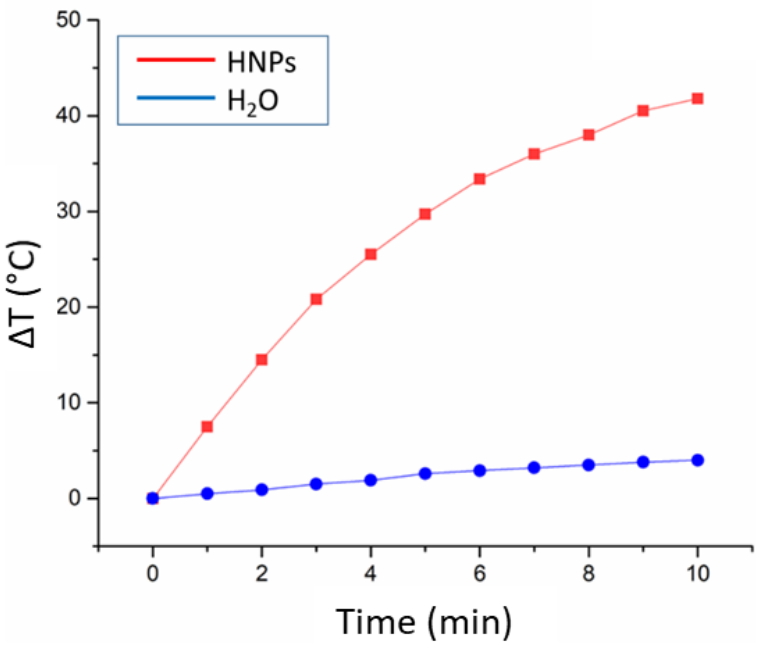

Figure 12: Photothermal results of nanocomposites after 10 minutes of laser irradiation. HNPs concentration: 0.1 mg/ml; Laser power: 1 W/cm^2.

Once characterized the sample in terms of size, morphology, chemical, magnetic and optical properties, a preliminary hemotoxicological analysis was performed in order to evaluate the toxicological effect of the nanocomposites in contact with red blood cells (RBCs). With this analysis it is possible to evaluate the hemoglobin absorbance using a

spectrophotometer, which is useful to detect the RBCs hemolysis before and after incubation with nanoparticles. The results concerning the RBCs hemolysis after incubation with 35 and 100 µg/ml concentration of HNPs, are shown in figure 13 in which it is possible to notice that after 5 h incubation, the HNPs did not show any hemotoxicity, which is comparable to that of the negative control sample. In fact, for each sample of RBC it is observed that the hemolysis is very low (lower than 1.4%), which means that the NPs hemotoxicity at these concentrations is negligible and therefore they are potentially usable for biomedical applications [52,53].

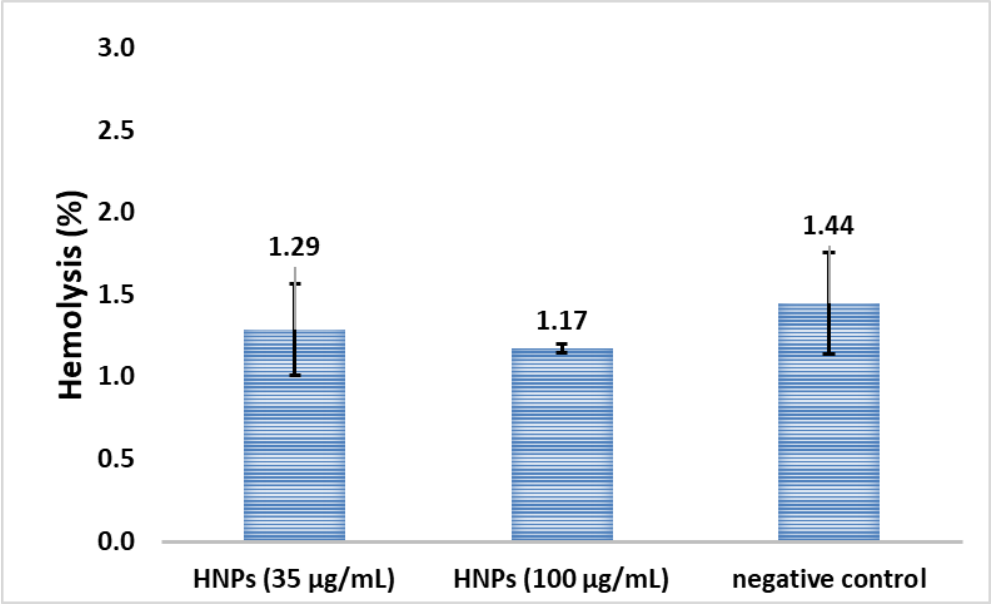

Figure 13: Hemotoxicity results. Cell viability of RBCs was evaluated after 5 h incubation at 37 °C (n=3). Data analysis revealed no statistically significant difference in cell viability values between tested groups ($p<0.05$).

4. Conclusions

In this this work a facile and reproducible synthesis method was optimized and used to develop new hybrid nanoplatforms composed by magnetic core and GNPs decoration. The

main goal was to prepare the HNPs through a green and simple synthesis by means of the innovative use of tannic acid, a polyphenolic compound as both reducing and stabilising agent. This approach allowed to prepare the HNPs without using any toxic chemical in the process, thus improving the synthesis procedure in terms of number of reagents used, properties, scalability, cost-efficiency and eco-sustainability. Further, another aim of the research was the complete characterization of the obtained HNPs including a preliminary hemotoxicological evaluation. The obtained structures are able to preserve the peculiar properties of each nanomaterial and display negligible hemotoxicity, creating a novel approach for magneto-photothermal therapy of cancer.

Acknowledgements

Authors are grateful for financial support from the Slovenian Research Agency ARRS (project number P2-0084) and to Elisa Bertone (DISAT) for FTIR and UV-Vis facilities.

Summary Points

- A facile and reproducible synthesis method was developed to prepare new hybrid nanoplatforms (HNPs) composed by magnetic core and gold nanoparticle decoration.
- The innovative use of tannic acid as both reducing and stabilising agent was used to prepare the HNPs
- The HNPs were prepared without any toxic chemical in the process.
- A complete characterization revealed that the obtained HNPs are able to preserve the peculiar properties of each nanomaterial.
- The obtained HNPs display negligible hemotoxicity.

- The obtained HNPs represent a novel approach for magneto-photothermal therapy of cancer.

References

[1] Jabir NR, Tabrez S, Ashraf GM, Shakil S, Damanhouri GA, Kamal MA. Nanotechnology-based approaches in anticancer research. *Int J Nanomedicin,* 7, 4391–408 (2012).

[2] Boisseau P, Loubaton B. Nanomedicine, nanotechnology in medicine. *Comptes Rendus Phys.* 12(7), 620–36 (2011). http://dx.doi.org/10.1016/j.crhy.2011.06.001

[3] Saini R, Saini S, Sharma S. Nanotechnology: the future medicine. *J Cutan Aesthet Surg.* 3(1), 32–3 (2010). https://www.ncbi.nlm.nih.gov/pubmed/20606992

[4] Holm BA, Bergey EJ, De T, Rodman DJ, Kapoor R, Levy L, et al. Nanotechnology in Bio Medical Applications. Molecular Crystals and Liquid Crystals. 374(1), 589-598 (2002) DOI: 10.1080/713738279

[5] Nikalje AP. Nanotechnology and its Applications in Medicine. *Med chem.* 5(2), 081-089 (2015).

[6] Boisseau P, Loubaton B. Nanomedicine, nanotechnology in medicine. *Comptes Rendus Phys.* 12(7),620–36 (2011). http://www.sciencedirect.com/science/article/pii/S1631070511001538

[7] Soares S, Sousa J, Pais A, Vitorino C. Nanomedicine: principles, properties, and regulatory issues. *Front Chem.* Article ID 6, 360, 15 pages (2018).

[8] Hwu JR, Lin YS, Josephrajan T, Hsu M, Cheng F. Targeted Paclitaxel by Conjugation to Iron Oxide and Gold Nanoparticles. *J. Am. Chem. Soc.* 131(1), 66–68 (2009).

[9] Kumar A, Boruah B, Liang X-J. Gold Nanoparticles: Promising Nanomaterials for the Diagnosis of Cancer and HIV/AIDS. *J Nanomater.* Article ID 202187, 17 pages (2011). https://doi.org/10.1155/2011/202187

[10] Shilpi S, Khatri K. Gold Nanoparticles as Carrier(s) for Drug Targeting and Imaging. *Pharm Nanotechnol.* 3(3),154-170 (2015).

[11] Huang X, El-Sayed MA. Gold nanoparticles: Optical properties and implementations in cancer diagnosis and photothermal therapy. *J Adv Res.* 1(1),13–28 (2010).

[12] Multari C, Miola M, Laviano F, Gerbaldo R, Pezzotti G, Debellis D, et al. Magnetoplasmonic nanoparticles for photothermal therapy. *Nanotechnology* 30(25), 255705 (2019). http://dx.doi.org/10.1088/1361-6528/ab08f7

[13] Gul S, Khan SB, Rehman IU, Khan MA, Khan MI. A comprehensive review of magnetic nanomaterials modern day theranostics. *Front Mater.* 6, Article179, 15 pages (2019).

[14] Bansal SA, Kumar V, Karimi J, Singh AP, Kumar S. Role of gold nanoparticles in advanced biomedical applications. *Nanoscale Adv.* 2(9), 3764–87 (2020).

[15] Kumar CSSR, Mohammad F. Magnetic nanomaterials for hyperthermia-based therapy and controlled drug delivery. *Adv Drug Deliv Rev.* 63(9), 789–808 (2011) http://dx.doi.org/10.1016/j.addr.2011.03.008

[16] Lodhia J, Mandarano G, Ferris N, Eu P, Cowell S. Development and use of iron oxide nanoparticles (Part 1): Synthesis of iron oxide nanoparticles for MRI. *Biomed Imaging Interv J.* 6, e12 (2010).

[17] Babes L, Denizot B, Tanguy G, Le Jeune JJ, Jallet P. Synthesis of iron oxide nanoparticles used as MRI contrast agents: a parametric study. *J Colloid Interface Sci.* 212(2), 474–82 (1999).

[18] Gobbo OL, Sjaastad K, Radomski MW, Volkov Y, Prina-Mello A. Theranostics Magnetic Nanoparticles in Cancer *Theranostics.* 5(11), 1249-63 (2015).

[19] Yoo D, Lee J-H, Shin T-H, Cheon J. Theranostic magnetic nanoparticles. *Acc Chem Res.* 44(10), 863–74 (2011).

[20] Chang D, Lim M, Goos JACM, Qiao R, Ng YY, Mansfeld FM, et al. Biologically Targeted Magnetic Hyperthermia: Potential and Limitations. *Front Pharmacol*; 9, Article 831, 20 pages (2018).

[21] Cheraghipour E, Javadpour S, Mehdizadeh A. Citrate capped superparamagnetic iron oxide nanoparticles used for hyperthermia therapy. *J Biomed Sci Eng.* 5(12), 715–719 (2012).

[22] Indira T. Magnetic Nanoparticles: A Review. *Int J Pharm*. 3(3), 1035–1042 (2010).

[23] Mahmoudi M, Serpooshan V, Laurent S. Engineered nanoparticles for biomolecular imaging. *Nanoscale.* 3(8), 3007–3026 (2011). http://dx.doi.org/10.1039/C1NR10326A

[24] Vinod M, Jayasree RS, Gopchandran KG. Synthesis of pure and biocompatible gold nanoparticles using laser ablation method for SERS and photothermal applications. *Curr Appl Phys.* 17(11), 1430–1438 (2017).

[25] Lucky SS, Soo KC, Zhang Y. Nanoparticles in Photodynamic Therapy. *Chem Rev.* 115(4), 1990–2042 (2015).

[26] Jain PK, Huang X, El-Sayed IH, El-Sayed MA. Noble metals on the nanoscale: optical and photothermal properties and some applications in imaging, sensing, biology, and medicine. *Acc Chem Res.* 41(12), 1578–1586 (2008).

[27] Zhang Y, Zhan X, Xiong J, Peng S, Huang W, Joshi R, et al. Temperature-dependent cell death patterns induced by functionalized gold nanoparticle photothermal therapy in melanoma cells. *Sci Rep.* 8(1), 8720 (2018). https://doi.org/10.1038/s41598-018-26978-1.

[28] Miola M, Ferraris S, Pirani F, Multari C, Bertone E, Žužek Rožman K, et al. Reductant-free synthesis of magnetoplasmonic iron oxide-gold nanoparticles. *Ceram Int.* 43(17),15258–65 (2017).

[29] de la Encarnación C, Lenzi E, Henriksen-Lacey M, Molina B, Jenkinson K, Herrero A, et al., Hybrid Magnetic–Plasmonic Nanoparticle Probes for Multimodal Bioimaging, *The Journal of Physical Chemistry C.* 126 (45), 19519-19531 (2022). DOI: 10.1021/acs.jpcc.2c06299

[30] Miola M, Multari C and a Vernè E, Iron oxide-Au magneto-plasmonic heterostructures: advances in their eco-friendly synthesis,

[31] *Materials.* 15, 7036 (2022). https://doi.org/10.3390/ma15197036

[32] Jadoun S, Arif R, Jangid NK, Meena RK. Green synthesis of nanoparticles using plant extracts: a review. *Environ Chem Lett.* 19(1), 355–74 (2021). https://doi.org/10.1007/s10311-020-01074-x

[33] Gupta H, Paul P, Kumar N, Baxi S, Das DP. One pot synthesis of water-dispersible dehydroascorbic acid coated Fe3O4 nanoparticles under atmospheric air: blood cell compatibility and enhanced magnetic resonance imaging. *J Colloid Interface Sci.* 430, 221–228 (2014). http://dx.doi.org/10.1016/j.jcis.2014.05.043

468 [34] Dahl JA, Maddux BLS, Hutchison JE. Toward greener nanosynthesis. *Chem*
469 *Rev.* 107(6), 2228–69 (2007).
470 *[35]* Gülçin İ, Huyut Z, , Elmastas M, Aboul-enein HY. Radical scavenging and
471 antioxidant activity of tannic acid. *Arabian Journal of Chemistry,* 3 (1), 43-53
472 (2010).
473 [36] Miola M, Multari C, Debellis D, Laviano F, Gerbaldo R, Vernè E, Magneto-
474 plasmonic heterodimers: Evaluation of different synthesis approaches, *J Am*
475 *Ceram Soc.* 105,1276–1285 (2022). DOI: 10.1111/jace.18190
476 [37] Ahmad T. Reviewing the Tannic Acid Mediated Synthesis of Metal
477 Nanoparticles. Thundat T, editor. *J Nanotechnol*. 2014, 954206 (2014).
478 https://doi.org/10.1155/2014/954206
479 [38] Gülçin İ, Huyut Z, Elmastaş M, Aboul-Enein HY. Radical scavenging and
480 antioxidant activity of tannic acid. *Arab J Chem.*3(1),43–53 (2010).
481 [39] Dong G, Liu H, Yu X, Zhang X, Lu H, Zhou T, et al. Antimicrobial and anti-
482 biofilm activity of tannic acid against Staphylococcus aureus. *Nat Prod Res.*
483 32(18),2225–2228 (2018). https://doi.org/10.1080/14786419.2017.1366485
484 [40] Martínez-Castañon GA, Nino-Martinez N, Martinez-Gutierrez F, Martinez-
485 Mendoza JR, Ruiz F. Synthesis and antibacterial activity of silver nanoparticles
486 with different sizes. *J nanoparticle Res.* 10(8), 1343–1348 (2008).
487 [41] Daduang J, Palasap A, Daduang S, Boonsiri P, Suwannalert P, Limpaiboon T.
488 Gallic acid enhancement of gold nanoparticle anticancer activity in cervical
489 cancer cells. *Asian Pac J Cancer Prev.* 16(1),169–74 (2015).
490 [42] de la Harpe KM, Kondiah PPD, Choonara YE, Marimuthu T, du Toit LC,
491 Pillay V. The Hemocompatibility of Nanoparticles: A Review of Cell-Nanoparticle

492 Interactions and Hemostasis. *Cells.* 8(10),1209 (2019). doi:
493 10.3390/cells8101209.
494 [43] Borroni E, Miola M, Ferraris S, Ricci G, Kristina Z, Kostevšek N, et al. Tumor
495 targeting by lentiviral vectors combined with magnetic nanoparticles in mice.
496 *Acta Biomaterialia.* 59, 303–316 (2017).
497 [44] Multari C, Miola M, Ferraris S, Movia D, Žužek Rožman K, Kostevšek N, et
498 al. Synthesis and characterization of silica-coated superparamagnetic iron oxide
499 nanoparticles and interaction with pancreatic cancer cells. *Int J Appl Ceram*
500 *Technol.* 15(4), 947–60 (2018).
501 [45] Bruce IJ, Taylor J, Todd M, Davies MJ, Borioni E, Sangregorio C, et al.
502 Synthesis, characterisation and application of silica-magnetite nanocomposites. *J.*
503 *Magn. Magn. Mater.* 284,145–160 (2004).
504 [46] Singh RK, Kim T-H, Patel KD, Knowles JC, Kim H-W. Biocompatible
505 magnetite nanoparticles with varying silica-coating layer for use in biomedicine:
506 Physicochemical and magnetic properties, and cellular compatibility. *J Biomed*
507 *Mater Res Part A.* 100A (7),1734–1742 (2012).
508 https://doi.org/10.1002/jbm.a.34140
509 [47] Pantoja M, González-Rodríguez H. Study by infrared spectroscopy and
510 thermogravimetric analysis of Tannins and Tannic acid. *Rev Latinoam química.*
511 39,107–12 (2010).
512 [48] Veisi H, Moradi SB, Saljooqi A, Safarimehr P. Silver nanoparticle-decorated
513 on tannic acid-modified magnetite nanoparticles (Fe_3O_4@TA/Ag) for highly
514 active catalytic reduction of 4-nitrophenol, Rhodamine B and Methylene blue.
515 *Mater Sci Eng C.* 100, 445–52 (2019).

[49] Aromal SA, Philip D. Facile one-pot synthesis of gold nanoparticles using tannic acid and its application in catalysis. *Phys E Low-dimensional Syst Nanostructures.* 44(7–8),1692–1696 (2012) http://dx.doi.org/10.1016/j.physe.2012.04.022

[50] Gold-nanoparticles-optical-properties. https://nanocomposix.com/pages/gold-nanoparticles-optical-properties. Cited 04/05/2023

[51] Correa JR, Bordallo E, Canetti D, León V, Otero-Díaz LC, Negro C, et al. Structure and superparamagnetic behaviour of magnetite nanoparticles in cellulose beads. *Mater Res Bull.* 45(8),946–53 (2010).

[52] Simmons M, Wiles C, Rocher V, Francesconi MG, Watts P. The preparation of magnetic iron oxide nanoparticles in microreactors. *J Flow Chem.* 3(1), 7–10 (2013).

[53] Ajdary M, Moosavi MA, Rahmati M, Falahati M, Mahboubi M, Mandegary A, et al. Health Concerns of Various Nanoparticles: A Review of Their in Vitro and in Vivo Toxicity. *Nanomater*. 8(9), 634 (2018).

[54] Yao Y, Zang Y, Qu J, Tang M, Zhang T. The Toxicity of Metallic Nanoparticles on Liver: The Subcellular Damages, Mechanisms, And Outcomes. *Int J Nanomedicine.* 14, 8787–804 (2019).